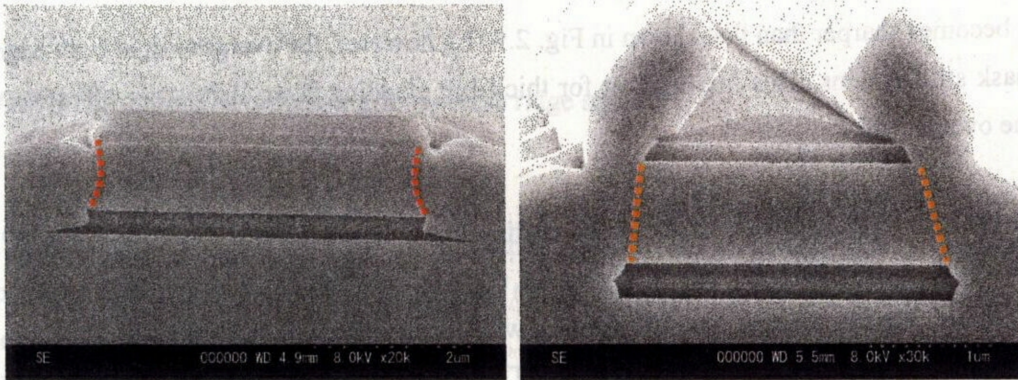

(a) Reverse ridge (b) Forward ridge

Fig.2.10 SEM images of the cross section view of the sample #4243. (a). for reverse ridge; (b) for forward ridge.

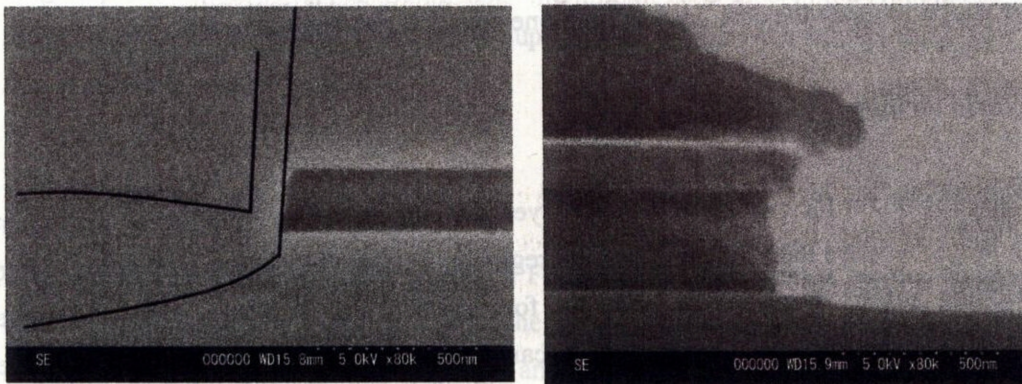

Fig. 2.11 SEM image of the cross section view of the samples. (a) #4094 after regrowth (b) #4042 before regrowth.

Fig. 2.10 shows the SEM image of the cross section view of the sample #4243 after regrowth for both reverse and forward ridge structure. Before regrowth, the samples were processed by ICP etching for InGaAs contact layer and InP cladding layer, followed by SBW wet etching for InGaAlAs core layer for reverse ridge type, as shown in Fig.2.10 (a), and by SH wet etching for forward ridge type, as shown in Fig.2.10(b). The sidewall of the InP is highlighted by brown dotted lines. In reverse ridge case, the sidewall etched by the ICP is as vertical as that etched by HCl, as shown in Fig. 2.9(a). No overgrowth occurs and the regrown region is almost at the same level as the active region. Note that short etching time of the core layer by SBW forms long tail stretching into the passive region. According to our previous consumption, no InGaAsP was grown on top of the tail. This can be improved by using citric acid or hybrid etching. Detailed discussion is given in the next subsection. In forward ridge case, the slope of the

sidewall becomes sharper than that shown in Fig. 2.9 (b), however, the overgrowth at both edges of the mask still remains. This implies that for thick InP cladding layer, ICP is not effective to cancel the overgrowth.

Fig. 2.11 shows the SEM image of the cross section view of the sample etched by only ICP before regrowth. In Fig.2.11 (a), the thickness of the InP cladding layer and InGaAs contact layer is 1200nm. We can see that the InP substrate was deeply etched by ICP. In Fig.2.11 (b), the thickness of the InP cladding layer is only 100nm. The undercut is caused by stain etching in SH for 5 seconds. The etching stopped almost exactly at the bottom of the core layer and only very thin substrate was etched. This is the best-controlled ICP etching in my experiments. Comparing the two figures with each other, we find that for thin layer etching, the etch depth can be precisely controlled. It shows the potential for precise control of the etch depth less than 1 um. ICP can be applied to etch the core layer in both one-step and two-step regrowth.

2.4.3.3 Hybrid etching

As mentioned above, for the etching of the core layer, dry etching suffers from the misalignment of the core layers between the active and passive region and uncertainty of the etch depth, while the wet etching suffers from severe undercut for reverse ridge structure. (Forward ridge structure is not suitable for one step regrowth because both wet etching and dry etching cause overgrowth, as mentioned in subsection 2.4.3.1). So in the next trial, we combine both of them.

The hybrid etching includes two steps: the first step is the dry etching of the most part of the core layer by ICP without suffering from severe undercut, and the second step is the wet etching of the remaining thin film of the core layer by selective chemical solution to form clear bottom interface. During the wet etching, the undercut can also been suppressed due to the quite short etch time determined by the thickness of the thin film.

For example, the optimized reverse ridge structure can be etched in the way shown in table 2.5.

Layer	Etching method	Contents
InGaAs	wet etching: for vertical and smooth sidewall	SH
InP		HCl
InGaAlAs	ICP dry etching: the top 300nm	
	Wet etching: the remain film	Citric acid (SBW:>30s)

Table 2.5 optimized processing for reverse ridge structure.

SBW is optional after the citric acid for smoother sidewall and weaker shadow effect. The etch time of SBW should be at least 30 second. Otherwise, it will bring more roughness.

2.4.4 two-step regrowth and one-step regrowth

Noticed from Fig.2.9 (d) that the forward ridge stucture has much better connection of the core layers between the active region and passive region. The main issue is its big horns due to its long slope of the cladding layer caused during wet etching processing step. Researchers have found that thin cladding layer can help to suppress the overgrowth significantly. This is why the 2-step regrowth was proposed.

Processing flow

The process for this technique is shown in Fig 2.12. The first step is the deposition of 200 nm SiO2 mask, followed by the definition of the passive region by photolithography. Then the thin non-intentionally doped InP cladding layer and MQW core layer in the passive region are etched by dry etching, wet etching or hybrid etching. In our case, the InP cladding layer is about 150 nm, thin enough to suppress the overgrowth without sacrificing diode performance. Then the first regrowth is carried out including the growth of the InGaAsP core layer and non-intentionally doped InP cladding layer in the passive region. After some treatment which is described in the next paragraph, the SiO2 mask in the active region is removed. Finally, the second regrowth takes place including the growth of the p-doped InP cladding layer and heavily p-doped InGaAs contact layer after other surface treatment.

Shadow effect reduction

While wet etching is used in the etching of InGaAlAs core layer, undercut happens more or less. In such case, the shadow effect can also be diminished by removing the stretched part of the cladding layer.

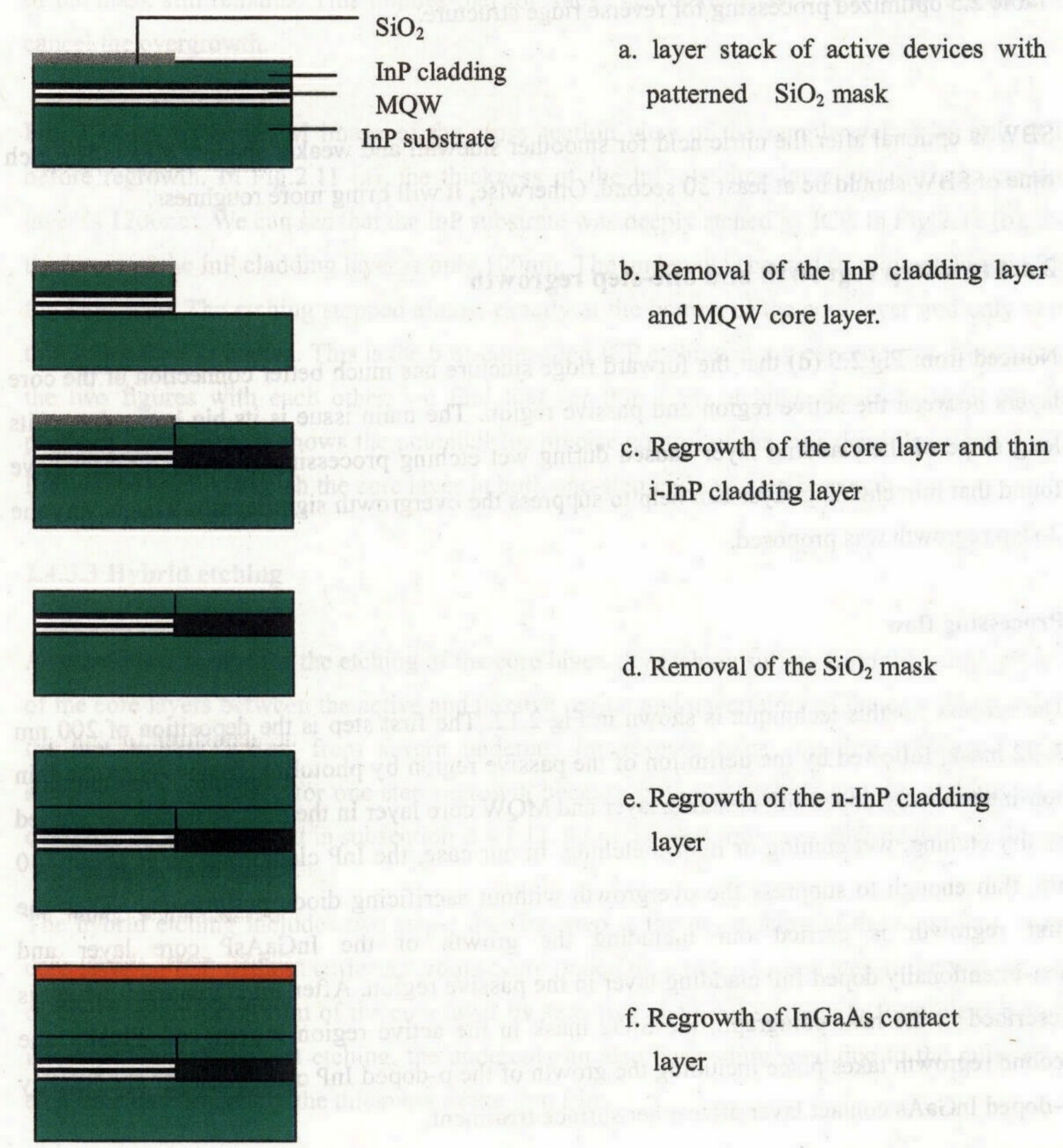

Fig. 2.12 two-step regrowth flow.

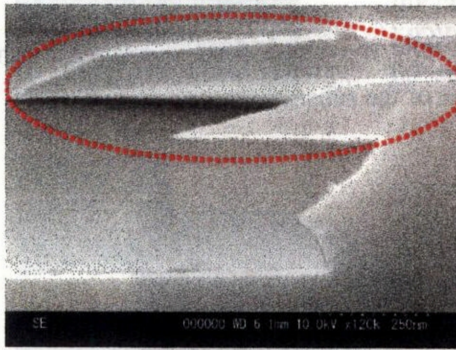
(a) before removal

(b) after removal

Fig. 2.13 Removal of the cladding wing before regrowth

Fig. 2.13 shows the SEM images of the cross section of the active region before and after removal of the cladding wings, as shown in Fig.2.13 (a) and Fig.2.13 (b) respectively. Due to the wet etching, both the cladding layer and core layer have undercut effect caused by their above layers, forming some wings (Fig. 2.13.a). This is the main reason for shadowing effect. In order to remove these wings, we put the sample into the BHF solution and then HCl solution. The etching time is determined by half of the total time to etch the corresponding layers. Seen from Fig. 2.13 (b), we find that the removal effectively shorten the stretched parts above the core layer.

Removal of overgrowth

In forward ridge case, slight overgrowth still happens, as shown in Fig. 2.14. Compared to Fig.2.7 (d), the overgrowth horns are thinner and narrower due to the thinning of the cladding layer.

In order to eliminate the effect of the overgrowth horns, two methods have been applied. One is to remove the overgrowth part by wet chemical means. Fig.2.15 shows the result after removing the SiO_2 mask and then 10 second immersion in the Saturated Bromine Water (SBW:HBr:H2O=1:5:10) solution. We can see that this method can effectively remove the overgrowth horns. However, the solution will also attack the cladding layer in the active region. So the thickness margin must be taken into account. Of course, SiO_2 mask can remain until the removal of the overgrowth region so as to protect the InP layer above the SCH. The second way is to obtain vertical sidewall of the core layer by using hybrid etching. Typically, we intend to etch the core layer till a 50-nm thin film remains. Since in the core layer, the etch rate of citric

acid at room temperature is about 100nm/min, one minute is enough for the etching of the remaining film and margin for cleaning the whole surface of the substrate.

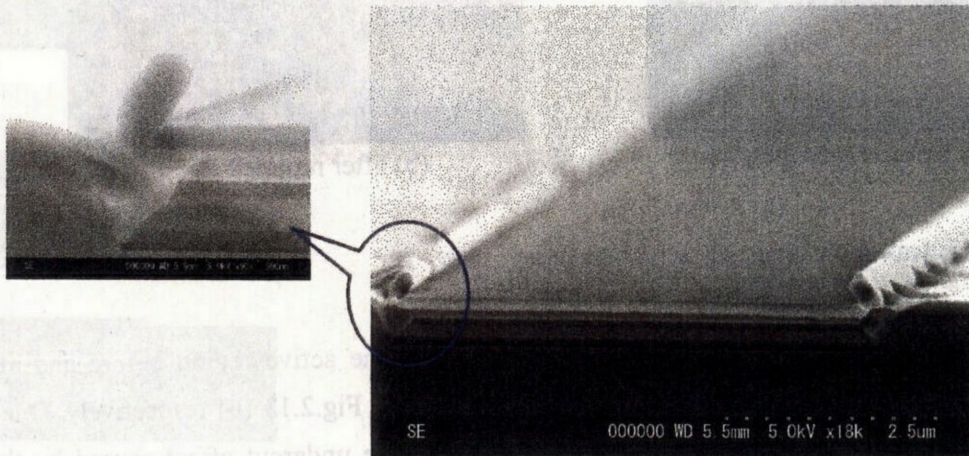

Fig.2.14 SEM images of the butt joint after the first step regrowth.

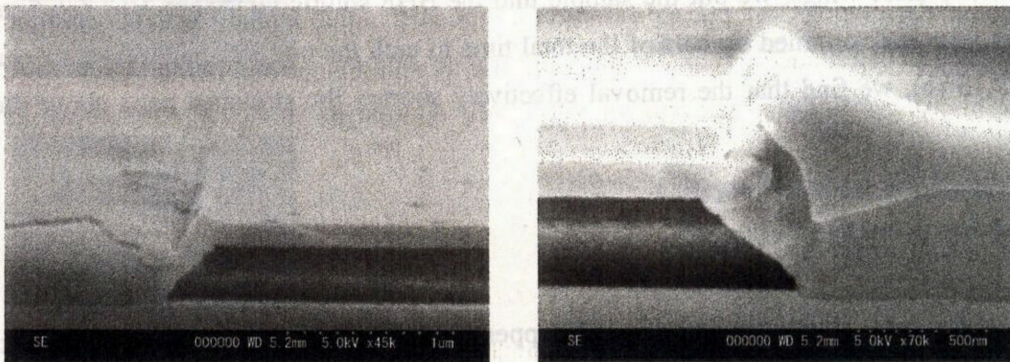

Fig. 2.15 SEM photographs of the butt joint. (a) top view. After removing the overgrowth horns and SiO_2 mask. (b) cross section view. Only removing the horns.

Based on the above experiments, we optimized the 2-step regrowth as shown in Fig.2.16. The main difference with Fig.2.12 lies in step (b~e). These steps are for the hybrid etching of the core layer and removal of the stretched edges. The step (c) and (d) are be omitted if the undercut has been greatly suppressed.

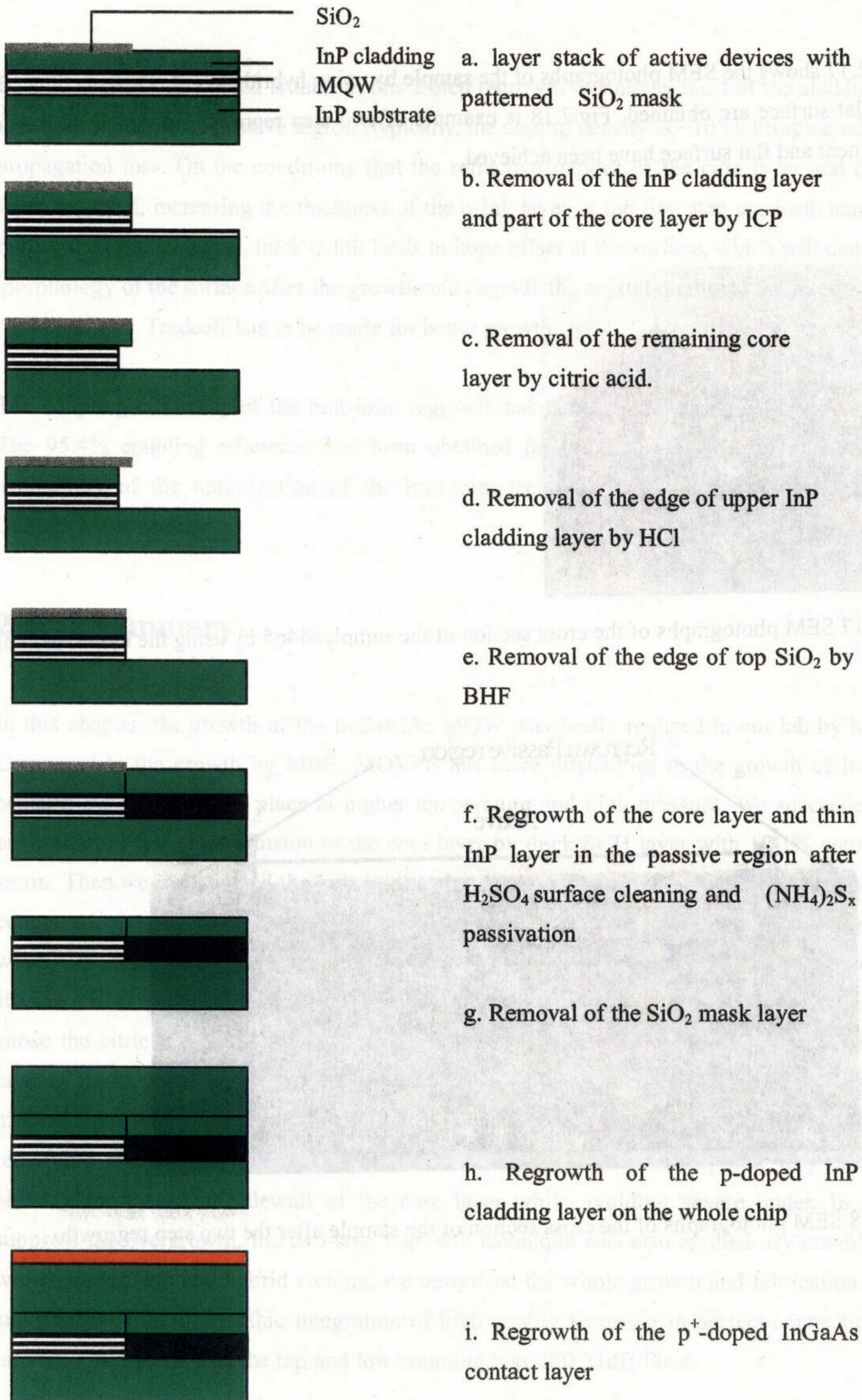

Fig. 2.16 Optimized 2-step regrowth flow

Fig. 2.17 shows the SEM photographs of the sample by using hybrid etching. Perfect connection and flat surface are obtained. Fig.2.18 is example of two-step regrowth, in which the vertical alignment and flat surface have been achieved.

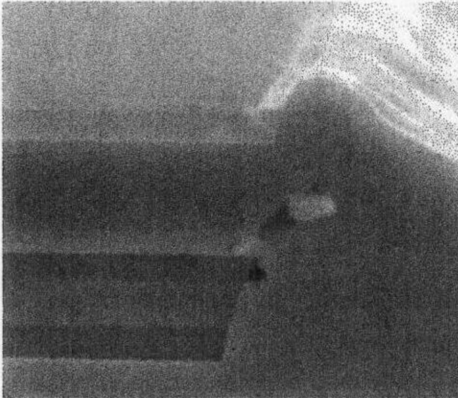

Fig.2.17 SEM photographs of the cross section of the sample#4465 by using the hybrid etching.

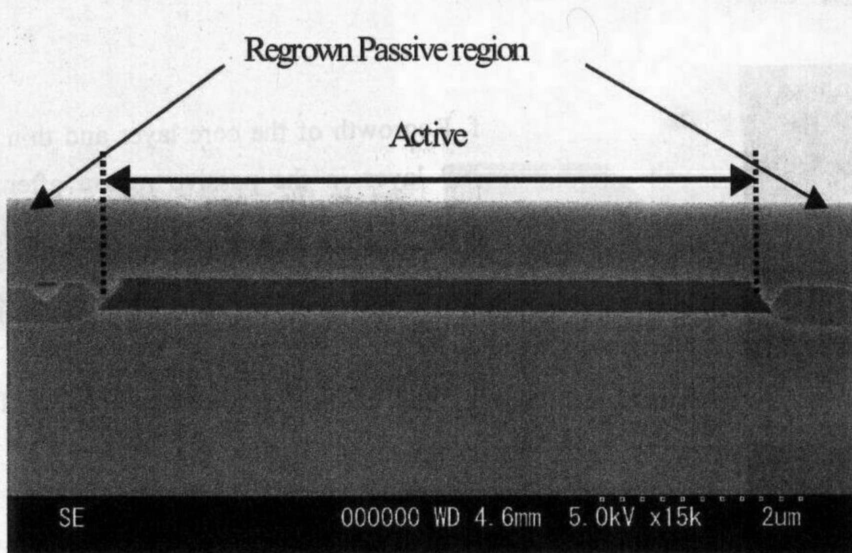

Fig. 2.18 SEM photographs of the cross section of the sample after the two step regrowth.

One thing need to be noted is that, in this 2-step regrowth technique, most of the cladding layer is p-type doped in the passive region (typically, the doping density is $\sim 10^{15}$), bringing additional propagation loss. On the conditions that the refractive indices of the core layer and cladding layer are fixed, increasing the thickness of the u-InP layer in the first step regrowth can help to reduce the loss. However, thick u-InP leads to large offset at the surface, which will degrade the morphology of the surface after the growth and degrade the crystal quality at the interface of the cladding layer. Tradeoff has to be made for better growth.

The coupling efficiency of the butt-joint regrowth has been measured in an all optical switch. The 95.4% coupling efficiency has been obtained for high mesa structure. It confirms the availability of the optimization of the butt-joint technique with ex-situ cleaning. Refer to Chapter V for details.

2.5 Summary

In this chapter, the growth of the InGaAlAs MQW was firstly realized in our lab by MOVPE. Compared to the growth by MBE, MOVPE has more difficulties in the growth of InGaAlAs because the growth takes place at higher temperature and high pressure. We succeeded in the prevention of the Zinc diffusion to the core layer by thick SCH layer with +0.1% compressive strain. Then we investigated the butt-joint technique by using ex-situ cleaning. As far as we are concerned, the butt-joint regrowth in the Al-containing materials remains a challenge in the word. The difficulties arise from several issues of this monolithic integration including the shadow effect, vertical alignment, Al oxidation and overgrowth. We tried several etchants and chose the citric acid as the best solution for achieving vertical profiles in the InGaAlAs core layer of EAM. An hybrid etching method was also proposed to avoid the undercut. This etching method starts with the ICP dry etching of most of the core layer, and then the wet etching of the remaining thin layer. SEM images confirmed that this hybrid etching was very effective to obtain almost vertical sidewall of the core layer while avoiding severe under. In order to suppress the overgrowth, the two-step regrowth technique was also applied. By combining the two-step regrowth and hybrid etching, we optimized the whole growth and fabrication process, and improved the monolithic integration of high quality featuring in perfect connection at the interface, flat surface on the top and low coupling loss of 0.21dB/facet.

References

[1] Foo Cheng Yit, "Fabrication of Monolithically Integrated Interferometer Switches by Selective Area MOVPE and their All-Optical Signal Processing Applications", Ph.D thesis, 2006

[2] N. Yoshimoto, Y. Shibata, S. Oku, S. Kondo, Y. Noguchi, K. Wakita, and M. Naganuma, "Fully polarization independent Mach-Zehnder optical switch using a lattice matched InAlGaAs/AlAlAs MQW and high-mesa waveguide structure," Electron. Lett., vol. 32, pp. 1368–1369,1996.

[3] St. Kollakowski, E. H. B¨ottcher, Ch. Lemm, A. Strittmatter, D. Bimberg, and H. Kr¨autle, "Waveguide-integrated InP-InGaAs-InAlGaAs MSM photodetector with very-high vertical coupling efficiency," IEEE Photon. Technol. Lett., vol. 9, pp. 496–498, 1997.

[4] Hiroyasu Mawatari, Mitsuo Fukuda, Shin-ichi Matsumoto, Kenji Kishi, and Yoshio Itaya, "Reliability and Degradation Behaviors of Semi-Insulating Fe-Doped InP Buried Heterostructure Lasers Fabricated by RIE and MOVPE", J. Light. Tech., Vol.15(3), pp.534-537, 1997

[5] R. Gessner, A. Dobbinson, A. Miler, J. Rieger, E. Veuhoff "Fabrication of AlGaInAs and GaInAsPburied heterostructure lasers by in situ etching", J.Cryst. Growth, Vol.248, pp426－430,2003,

[6] Y.Muroya, T.Okuda, R.Kobayashi, K.Tsuruoka,Y.Ohsawa, T.Koui, T.Tsukuda, T.Nakamura, "100°C, 10-GbIs Direct Modulation with a Low Operation Currenl of 1.3-pm AlGalnAs Buried Heterostructure DFB Laser Diodes", OFC03, FG7,pp684, 2003

[7] Sun HD, Macaluso R, Dawson MD, et al. "Characterization of selective quantum well intermixing in 1.3 mu m GaInNAs/GaAs structures," J APPL PHYS vol.94, no.3, pp.1550-1556, 2003.

[8] Ng SL, Djie HS, Lim HS, et al., "Fabrication of wide-band electro-absorption waveguide modulator arrays using quantum well-intermixing process," OPT COMMUN , vol.226: (1-6), pp.191-197, OCT 15, 2003.

[9] R. Gessner, A. Dobbinson, A. Miler, J. Rieger, E. Veuhoff "Fabrication of AlGaInAs and GaInAsPburied heterostructure lasers by in situ etching", Journal of Crystal Growth, Vol.248, pp.426–430, 2003

[10] T. Kitatani, K. Shinoda, T. Tsuchiya, H. Sato, K. Ouchi, H. Uchiyama, S. Tsuji, and M.

Aoki, "Evaluation of the Optical-Coupling Efficiency of InGaAlAs–InGaAsP Butt Joint Using a Novel Multiple Butt-Jointed Laser", PHOTONICS TECHNOLOGY LETTERS, Vol.17(6), pp.1148-1150, 2005

[11] J. Shimizu, M. Shirai, M. Aoki, "InGaAlAs selective-area growth on an InP substrate by metalorganic vapor-phase epitaxy T. Tsuchiya", Journal of Crystal Growth, Vol.276, pp. 439–445, 2005

[12] Jung-Ho Song, Jung-Woo Park, Eun-Deok Sim, and Yongsoon Baek, "Measurements of Coupling and Reflection Characteristics of Butt-Joints in Passive Waveguide Integrated Laser Diodes", PHOTONICS TECHNOLOGY LETTERS, Vol.17(9), pp.1791-1793, 2005

[13] DESALVO, G.C., W.F. Tseng, and J. Comas, "Etch Rates and Selectivities of Citric Acid/H_2O_2 on GaAs, $Al_{0.3}Ga_{0.7}As$, $In_{0.2}Ga_{0.8}As$, $InGa_{0.53}Ga_{0.47}As$, $In_{0.52}Ga_{0.48}As$ and InP," J. Electrochem. Soc., Vol.139(3), pp.831~835, 1992